An Underwater Target Detection System for Electro-Optical Imagery Data

Michael Kabatek*, Mahmood R. Azimi-Sadjadi*, and J. Derek Tucker*†
*Department of Electrical and Computer Engineering
Colorado State University, Fort Collins, Colorado 80523-1373
Email: {makabatek,azimi,dtucker}@engr.colostate.edu
†Naval Surface Warfare Center - Panama City Division
Panama City, FL 32407-7001
Email: james.d.tucker@navy.mil

***Abstract*—The problem of detecting underwater targets from Electro-optical (EO) images is considered in this paper. A block-based log-likelihood ratio test has been developed for detection and segmentation of underwater mine-like objects in the EO images captured with a CCD-based image sensor. The main focus of this research is to develop a robust detection algorithm that can be used to detect low contrast and partial underwater objects from the EO imagery with low false alarm rate. The detection method involves identifying frames of interest (FOI) containing the potential targets. Once the FOI have been identified, regions of interest (ROI) within the FOI are segmented from the background. Performance of the detection method is tested in terms of probability of detection, false alarm rate, and receiver operating characteristic (ROC) curves for FOI in the selected data runs. The algorithm shows promising results in target detection and generation of good silhouettes for subsequent classification.**

***Index Terms*—Binary hypothesis testing, electro-optical sensors, underwater target detection**

I. Introduction

Automatic detection and recognition of underwater objects from EO imagery poses a serious challenge due to poor environmental and operating conditions that impair the quality of the captured images. Although the sensor technology for underwater mine identification has advanced to a level that these systems are being transitioned into the fleet, the target identification is still being done by human operators [1]. The development of an automatic underwater target identification system capable of identifying various types of underwater targets, under different environmental conditions pose many technical problems. Some of the contributing factors are: Targets have diverse sizes, shapes and reflectivity properties. Target emplacement environment is variable; targets may be proud or partially buried. Environmental properties vary significantly from one location to another. In particular, the variation in the turbidity can substantially change the quality of the collected data and hence the conspicuity of the targets. Bottom features such as sand, rocks, corals, and vegetation can conceal a target whether it is partially buried or proud. Competing clutter with responses that closely resemble those of the targets may lead to false positives. All these factors contribute to make this problem a very complicated one.

Previous work on EO data has been focused on Streak Tube Imaging Lidar (STIL) system [1]–[4], and laser line scan (LLS) [5]–[7] based systems. STIL sensor produces high-resolution 3-D images of underwater objects by scanning (line by line), on the target field [1]. The collected raw STIL data is rendered to produce pairs of contrast (gray-level) and range (distance) maps. The previous work focuses on filtering, segmentation, and classification of underwater mine-like objects from pre-cropped regions of the STIL scans.

In this paper we present the development of a block-based log-likelihood detector for use with a EO imagery database different than that produced by the STIL EO sensor. This database was collected using a new CCD EO system capable of producing ocean bottom snapshot images. The new CCD EO system is contained inside the Bluefin 12 underwater unmanned vehicle (UUV) developed by Bluefin Robotics Corp. and is capable of capturing subsequent snapshots over a target field as the vehicle is moving. The proposed detector is capable of identifying frames of interest (FOI) which contain potential targets within data runs produced by the CCD sensor, as well as segmenting the regions of interest (ROI) from the detected frames. An important benefit of the proposed detector lies in the fact that detection of FOI and ROI segmentation can be achieved in a single step. FOI detection followed by automatic ROI segmentation will reduce the number of objects from which features need to be extracted, as well as reduce the overall processing load on the classifier.

This paper is organized as follows: In Section II we will discuss the CCD sensor and its properties. Section III describes the sensor data and challenges associated with detecting objects from this EO database. Section IV discusses the design and implementation of the block-based detector. Section V assesses the performance of the detector on the EO database. Finally, Section VI gives conclusions on this work and discusses future work.

II. CCD Sensor Description & Properties

This section provides an overview of the data collected by the CCD system. The sensor used in this work employs a DVC 1500 monochrome CCD camera coupled with a Philips Lumiled Luxeon Flood 18 LED illuminator [8]. The illuminator has a luminous flux > 500 lumens, and the CCD camera is capable of producing images of sizes 1394 x 1040 (6.45um

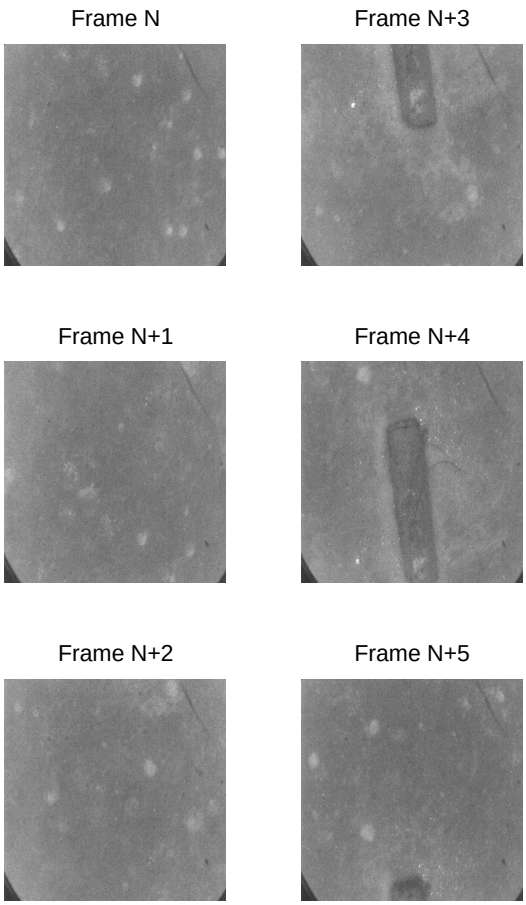

Fig. 1. A sequence of frames from run TargetY8_001 containing target frames (both full and partial targets).

pixel size) with gray level resolution of 12-bit/pixel. The camera also supports multiple binning modes (1x1 to 8x8) [8]. An example of a frame sequence is shown in Figure 1. The focus of this work is to separate the frame(s) of interest (FOI), which contain potential targets from those that do not contain targets. The second objective is to segment the mine-like object within an FOI from the background in order to classify it as target or non-target. As mentioned the CCD sensor takes several ocean bottom snapshots in a run making the detection process different from the previous work [1], [2]–[4], [8], [9] on EO images.

III. CCD Sensor Data & Challenges

The CCD image data consists of a series of ocean bottom snapshots as in Figure 1. The data analyzed in this study consisted of five data runs containing targets, and five containing no targets (just background). The data runs used together with total number of frames per run and target FOI's are given in Table I.

TABLE I
TESTED CCD DATA SET

Run	Total Frames	Target Frames
SAM001_003	42	0
SAM004_001	35	0
SAM22_011	35	0
SAM23_003	293	3
SAM23_004	287	3
SAM23_005	293	4
TargetY8_001	136	3
TargetY8_003	29	0
TargetY8_004	32	0
TargetY8_006	135	3
Totals	1317	16

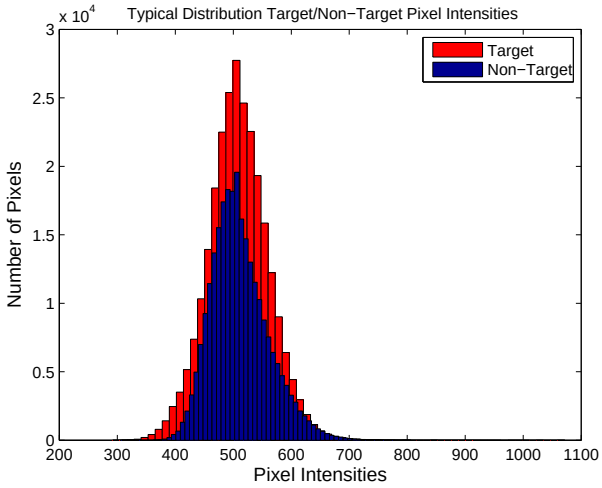

Fig. 2. Histograms of typical Target and Non-Target frames.

As can be seen the total number of frames in the data runs is 1317, of which 16 frames contain targets. For these data runs the CCD system was set to produce images that are 684x513 pixels at 12-bits per pixel gray level resolution. The data imported is resized to 512x512 pixels for ease of computation using MATLAB bicubic interpolation image resizing algorithm. Example data frames containing target (frames N+3, N+4, N+5) and non-target (frames N, N+1, N+2) are shown in Figure 1. The data set contains only three different types of targets namely cylindrical, circular, and trapezoidal targets.

There are three main tasks involved in designing an automatic target detection and recognition system for this new EO database. The first is FOI detection, which is the key to the success of other subsequent processing steps namely feature extraction and classification. Since only a few out of several hundred frames in a run may contain a partial or full target images, it is important to isolate only those frames which contain a potential target from those of background. The next task is segmentation of the objects within the FOI for ROI selection. This is also critical due to the fact that background and mine-like objects tend to have very similar contrast characteristics, hence making the segmentation and

discrimination very difficult tasks. The third task involves designing the classification system. The challenge of the detector and classifier for this new CCD EO database lies in the fact that FOI may contain partial targets (e.g. see frame N+3 and N+5 in Figure 1). Partial targets cause difficulties in both detection and classification processes due to the fact that the extracted ROI may not contain adequate information. The challenges and issues in these tasks are discussed in more detail below.

1) As mentioned before each data run contains a large number of frames containing only background and few frames containing targets. The focus of this work is to detect FOI within the runs, and extract ROI only from the detected frames containing potential targets. Once ROI are extracted from the FOI, the problem becomes a two-class classification problem to determine if the detected object is a target or a non-target. The main challenge involves designing a detector that will provide screening mechanism to filter out any frames that have no object of interest. If a target exists in a frame, the frame must be marked as FOI, so that the detected objects contained in the FOI can be classified.
2) The next main challenge when designing a detection system for this new EO database is successful ROI segmentation. We can see from typical target and background frames in Figure 1 and histogram of example frames (Target N+4 and Non-target N+1) in Figure 2 that the background and target have overlapping gray level intensities. This makes it difficult to employ global-based schemes to segment the detected objects. Also the CCD EO images do not provide any identifiable texture to allow discrimination between target and background.
3) Finally partial targets are fragmented ROI within a FOI. This can occur because of occlusion or when only a portion of a target is captured in a frame, hence causing two problems. The first problem is the fact that a partial target may be very small and indistinguishable from background anomalies. Small objects pose a challenge since the detector must have some way of discriminating small anomalies from very small portions of targets. Another issue involved in partial targets exists in the fact that these small ROI must be classified after they are detected. A classifier may incorrectly classify a partial target due to the lack of discriminatory information of the mine-like object.

IV. Block-Based Detection

In this section the proposed block-based method for detection of FOI within a run, and determining ROI within the detected frames is described. The main reason for taking a local-based (block) approach as opposed to a global-based approach employed in [1], [5], [10] lies in the fact that FOI must be determined for every data run. If a histogram (global-based) approach were to be employed here preprocessing and segmentation would be performed on every frame in the data set. However, as mentioned before in the CCD-based database mine-like objects tend to have very similar pixel intensity as those of background regions, hence making global-based methods inefficient for this application. In contrast, in the local block-based approach each image is processed block-by-block using a local-based Gauss-Gauss detector [11], [12] which exploits local statistical properties of the target and non-target blocks.

Only blocks that have similar characteristics to targets are flagged as detections. Once all blocks within a given frame are processed then a collection of connected blocks will be defined. Conceivably this method should identify all the blocks in a given frame that belong to a potential target. This collection of connected blocks will result in a segmented target from which features will be extracted. The proposed local-based method accomplishes two goals: (1) determines if an object (or part of an object) exists in a frame thereby detecting a FOI (This reduces the number of frames which need to be looked at by the classifier); and (2) automatically gives the location of the potential target by segmenting the ROI with mine-like characteristics from the FOI. In what follows, we describe the theory and results of this block-based detector.

A. Review of Binary Hypothesis Testing

The classical detection problem of choosing between two hypotheses [11] is that given an N-dimensional observation space, where $\mathbf{x} = [x_1, x_2, \cdots, x_N]^H$ represents an observation vector in this space, we would like to test between H_1 hypothesis (true) and H_0 hypothesis (null) for this observation vector. Clearly, each time we conduct the test there are four possible outcomes that are: (a) H_0 is true and we choose H_0, (b) H_0 is true and we choose H_1, (c) H_1 is true and we choose H_1, and (d) H_1 is true but we choose H_0. The first and third outcomes lead to correct decisions while the second and fourth outcomes lead to erroneous decisions. The Bayes test is based on two assumptions. First, the two hypotheses, H_0 and H_1, correspond to two possible prior probabilities, P_0 and P_1, respectively. These probabilities represent the prior observer's information about the hypotheses before the detection is conducted. The second assumption is that there is a cost associated with each of the four courses of action described above. These costs are denoted by, C_{00}, C_{10}, C_{11}, and C_{01}, for outcomes 1-4, respectively. It is assumed that the cost of a wrong decision is higher than the cost of a correct decision, i.e. $C_{10} > C_{00}$ and $C_{01} > C_{11}$. The goal of the Bayes test is to design a decision rule so that on the average cost of a decision will be as small as possible, which subsequently leads to the smallest Bayesian risk when making the decision.

Because the decision rule is binary, i.e. there are only two possibilities, either H_0 and H_1, we can view the rules as a division in the observation space into two parts A_0 and A_1. In other words, if the observation is found in the region A_0 the hypothesis H_0 is declared true and if the observation is found in the region A_1 the hypothesis H_1 is declared true. By viewing the problem in this manner we express [11] the risk

$\mathcal{R}$ in terms of the decision regions and probabilities as,

$$\begin{aligned}\mathcal{R} &= C_{00}P_0\int_{A_0} p_{\mathbf{X}|H_0}(\mathbf{x}|H_0)\,d\mathbf{x} \\ &+ C_{10}P_0\int_{A_1} p_{\mathbf{X}|H_0}(\mathbf{x}|H_0)\,d\mathbf{x} \\ &+ C_{11}P_1\int_{A_1} p_{\mathbf{X}|H_1}(\mathbf{x}|H_1)\,d\mathbf{x} \\ &+ C_{01}P_1\int_{A_0} p_{\mathbf{X}|H_1}(\mathbf{x}|H_1)\,d\mathbf{x}. \end{aligned} \quad (1)$$

where $p_{\mathbf{X}|H_i}(\mathbf{x}|H_i)$ is the conditional probability density of observation given hypothesis H_i, $i = 0, 1$. To find the decision rule, the decision regions are determined such that the risk in (1) is minimized. Because each element of $\mathbf{x}$ must be assigned to either the A_0 or A_1 in the observation space A, we can say that $A = A_0 \cup A_1$ and $A_0 \cap A_1 = \emptyset$. Now, if we use $\int_A p_{\mathbf{X}|H_0}(\mathbf{x}|H_0)\,d\mathbf{x} = \int_A p_{\mathbf{X}|H_1}(\mathbf{x}|H_1)\,d\mathbf{x} = 1$, then (1) can be rewritten [11] as,

$$\begin{aligned}\mathcal{R} &= P_0C_{10} + P_1C_{11} \\ &+ \int_{A_0}[P_1(C_{01} - C_{11})p_{\mathbf{X}|H_1}(\mathbf{x}|H_1) \\ &- P_0(C_{10} - C_{00})p_{\mathbf{X}|H_0}(\mathbf{x}|H_0)]\,d\mathbf{x} \end{aligned} \quad (2)$$

The first two terms in (2) represent the fixed cost and the integral represents the cost controlled by the points in the observation space, A that are assigned to A_0. The points in A for which the first term in the integral which are larger than the second term are assigned to A_1, whereas the points in which the second term is larger than the first term are assigned to A_0. Any points in which the terms are equal have no effect on the cost and can be arbitrarily assigned to any region (we assume that the points are assigned to A_1). We can, therefore, define the decision region in the observation space by

$$\frac{p_{\mathbf{X}|H_1}(\mathbf{x}|H_1)}{p_{\mathbf{X}|H_0}(\mathbf{x}|H_0)} \underset{H_0}{\overset{H_1}{\gtrless}} \frac{P_0(C_{10} - C_{00})}{P_1(C_{01} - C_{11})}. \quad (3)$$

The quantity on the left is called the *likelihood ratio* and will be denoted by

$$l(\mathbf{x}) \triangleq \frac{p_{\mathbf{X}|H_1}(\mathbf{x}|H_1)}{p_{\mathbf{X}|H_0}(\mathbf{x}|H_0)}. \quad (4)$$

The relationship on the right is the threshold of the test and will be denoted by η. Thus, Bayes criterion leads to a likelihood ratio test,

$$l(\mathbf{x}) \underset{H_0}{\overset{H_1}{\gtrless}} \eta. \quad (5)$$

Our proposed method for hypothesis testing is based on the Neyman-Pearson criterion [11], in which the hypothesis test is formulated as a constrained optimization problem. In this optimization problem the false alarm probability is constrained and the probability of detection is maximized. The optimization problem yields a likelihood ratio test and thresholding conditions. The Neyman-Pearson criterion [11], [13] generates a test to maximize P_d (probability of detection) while making P_{fa} (probability of false alarm) as small as possible. The criterion constrains $P_{fa} = \alpha' \leq \alpha$ and designs a test that maximizes the probability of detection under this constraint [11].

We applied a block-based likelihood ratio test using the standard Gauss-Gauss detector [12] which is used to determine if a block belongs to a potential target or just background. The detection problem is viewed in terms of the signal plus noise model [12], [13], the decision between two hypotheses is now either background (noise) only (H_0) or target (signal) plus background (H_1). Assuming that observation block of size NxN shaped column-wise into a vector $\mathbf{x} \in \mathbb{R}^{N^2}$ is Gaussian distributed with zero-mean and covariance matrix R. We test the hypothesis $H_0 : R = R_0$, i.e. noise alone versus $H_1 : R = R_1$, i.e signal plus noise where $R_1 = R_0 + R_s$, R_0 is the covariance matrix of the noise alone, and R_s is the covariance matrix of the target alone. It is assumed that noise and target are uncorrelated. Thus, the conditional probability density function for a given hypothesis $H_i,\ i \in [0, 1]$ and a given observation vector $\mathbf{x}$ is given by

$$p_{\mathbf{X}|H_i}(\mathbf{x}|H_i) = (2\pi)^{-\frac{N^2}{2}}|R_i|^{-\frac{1}{2}}e^{-\frac{1}{2}\mathbf{x}^H R_i^{-1}\mathbf{x}}. \quad (6)$$

where $p_{\mathbf{X}|H_i}(\mathbf{x}|H_i)$ is the conditional probability of $\mathbf{x}$ given H_i, $i \in [0, 1]$.

Using the likelihood ratio in (4) and taking the natural log, the log-likelihood of $\mathbf{x}$ becomes [12]:

$$\begin{aligned} l(\mathbf{x}) &= ln\left(\frac{(2\pi)^{-\frac{N^2}{2}}|R_1|^{-\frac{1}{2}}e^{-\frac{1}{2}\mathbf{x}^H R_1^{-1}\mathbf{x}}}{(2\pi)^{-\frac{N^2}{2}}|R_0|^{-\frac{1}{2}}e^{-\frac{1}{2}\mathbf{x}^H R_0^{-1}\mathbf{x}}}\right) \\ &= ln\left(\frac{|R_1|^{-\frac{1}{2}}}{|R_0|^{-\frac{1}{2}}}e^{\frac{1}{2}\mathbf{x}^H\left(R_0^{-1} - R_1^{-1}\right)\mathbf{x}}\right) \\ &= \frac{1}{2}ln|R_0| - \frac{1}{2}ln|R_1| + \frac{1}{2}\mathbf{x}^H\left(R_0^{-1} - R_1^{-1}\right)\mathbf{x} \end{aligned}$$

Disregarding the constants that are not observation dependent, the likelihood-ratio for the Gauss-Gauss detector [12] becomes

$$\begin{aligned} l(\mathbf{x}) &= \mathbf{x}^H\left(R_0^{-1} - R_1^{-1}\right)\mathbf{x}. \\ &= \mathbf{x}^H Q\mathbf{x}. \end{aligned} \quad (7)$$

Where $Q = R_0^{-1} - R_1^{-1}$ Defining

$$\begin{aligned} \mathbf{y} &= R_0^{-1/2}\mathbf{x} \\ S &= R_0^{-1/2}R_1R_0^{-T/2} \end{aligned} \quad (8)$$

Where S is the "Signal-to-noise ratio" matrix [12], the log-likelihood in 8 ratio now takes the form:

$$l(\mathbf{x}) = \mathbf{y}^T(I - S^{-1})\mathbf{y} \quad (9)$$

Now, if we express S in terms of it's orthogonal decomposition $S = U\Lambda U^T$ where $\Lambda = diag[\lambda_1 ... \lambda_N]$ contains the eigenvalues of S, and U contain the associated eigenvectors. The log-likelihood ratio becomes

$$l(\mathbf{x}) = \mathbf{y}^T U(I - \Lambda^{-1})U^T\mathbf{y} \quad (10)$$

If $\lambda_1 > \lambda_2 > ... > \lambda_r > \lambda_{r+1} > ... > \lambda_N$, then the reduced rank version of (10) can be written as

$$l_r(\mathbf{x}) = \mathbf{y}^T U(I_r - \Lambda_r^{-1})U^T\mathbf{y} \tag{11}$$

Where Λ_r and I_r are the reduced rank version of I and Λ^{-1} containing r non-zero entries. Using this rank r log-likelihood ratio, (for $r = 1$) is implemented for each block to determine if the block belongs to a target.

B. Detector Design

In order to use the proposed block-based likelihood detector a training set must be used to design the detector. The selection of a set of blocks from targets and background is required. This process is subjective in that the blocks used for the training must be specifically picked from frames which are believed to represent a wide range of targets. Since a limited number of frames containing targets are available in this database, blocks from a two data runs (TargetY8_001 & SAM002_008) containing targets were used. In order to form the training set, regions of target and background were cropped from the frames shown in Figure 3.

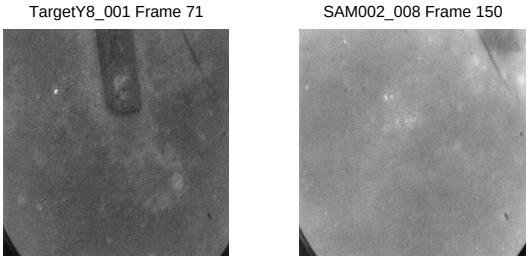

Fig. 3. FOI from data runs TargetY8_001 & SAM002_008 used to train the Gauss-Gauss detector. Regions of blocks were selected over the target and background regions.

More specifically, two sets each containing 1465 blocks each (2930 blocks total) were selected from the two data runs TargetY8_001 & SAM002_008 for target and non-target regions to form covariance matrices R_1 and R_0, respectively. These were selected so that they only contain target or non-target pixels, and boundary regions. The covariance matrices R_1 and R_0 are then formed by rearranging the blocks into vectors and computing the sample covariance matrices. After training the detector was evaluated on the entire data set in Table I in order to evaluate the performance for FOI detection.

A log-likelihood threshold needs to be chosen in order to differentiate between background and target blocks. This threshold value was experimentally chosen to be 5 based on analyzing several different blocks over both target and non-target regions. It turns out that this threshold is adequate for most of the data sets.

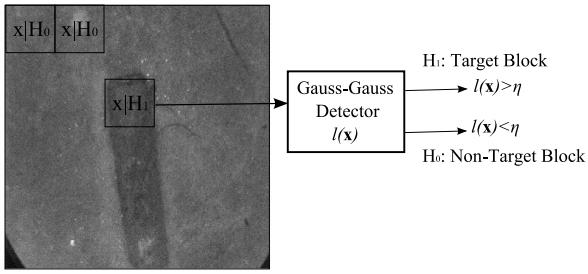

Fig. 4. Block-based detection process.

C. Implementation of Block-based Detection

Each frame in a data run is partitioned into blocks of size 4x4 pixels. Each block is then rearranged into a vector for computing the log-likelihood ratio. An exaggerated example of the blocking is shown in Figure 4.

The Gauss-Gauss detection is then performed on each block, and a likelihood value is computed. This generates a 'likelihood map' image. In this likelihood map image each pixel represents the value of the log-likelihood ratio of the corresponding block in the EO image. The likelihood maps are then used to determine both FOI and ROI in a data set based on thresholding the log-likelihood ratio. This log-likelihood ratio thresholding is based on the training frames from runs TargetY8_001 & SAM002_008 .

At least 25 connected blocks must be detected in order for the frame to be flagged as a FOI. Also an upper size threshold on the number of connected blocks may be imposed. If too many connected blocks are detected then the frame is assumed to contain only background. These size constraints pose another challenge to the FOI detector. If the vehicle carrying the sensor is high above the targets, the targets may appear small, and may be missed due to the lower size threshold, conversely if the vehicle is directly over the target then the target may appear too large. The size constraints were determined experimentally using the different targets in the database to be 25 to 2500 blocks. The overall process is described in the following steps:

1) Apply the likelihood ratio at each block using the Gauss-Gauss formulation in (5) and (8).
2) If the block's likelihood ratio falls below the pre-specified threshold then designate the particular block as 'target' otherwise the block is declared as a background block.
3) Determine the number of connected blocks and impose the minimum and maximum number constraints and flag the frame under consideration as a FOI if all required conditions are met.

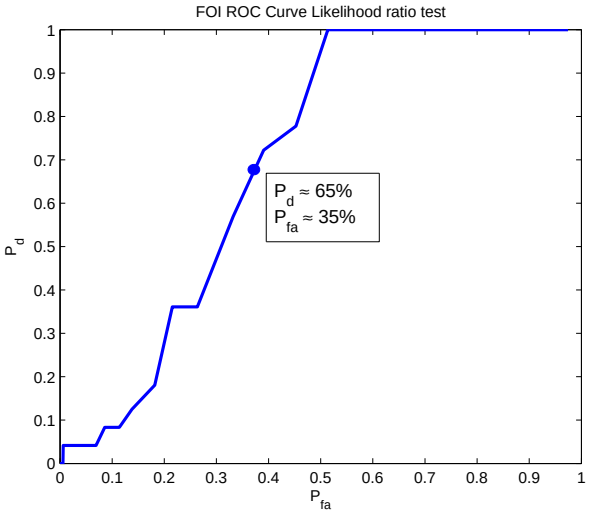

Fig. 5. FOI ROC curve for the data set shown in Table I using 4x4 blocks.

V. Detection Results

Using the log-likelihood ratio test for FOI detection the receiver operating characteristic (ROC) curve was generated for the data set in Table I. The ROC shown in Figure 5 represents the FOI detection results, which show how many frames are detected as false alarm compared to actual targets. This ROC is based on 'object' detection, i.e. if an object of 25 or more connected blocks is detected the frame is flagged as a detected frame (or FOI). This ROC gives an indication of the number of FOI detected per run. This ROC also give an indication of how many frames are pre-filtered or removed for the classification stage. Once a frame is flagged as FOI, the ROI of the mine-like object is segmented for feature extraction by way of the detected connected blocks. Higher false alarm rates during FOI detection requires the overall system to perform unnecessary feature extraction and slows down the classification on the entire run. The block-based log-likelihood scheme was evaluated on the data set for 4x4 blocks for FOI detection. At the knee point of ROC where $P_d + P_{fa} = 1$, we have $P_d \approx 65\%$ and $P_{fa} \approx 35\%$. This result may appear disappointing but it shows that for $P_d = 1$ all frames containing potential objects are detected, while on average half the frames from the run are eliminated from the classification stage. Eliminating frames from the classification stage will ultimately reduce the load on the classifier. Several detection results based upon 4x4 block size detector are shown in Figures 6 (a)-(c). The three cases shown correspond to an easy, a medium, and a difficult target case respectively. The examples are given for the pre-specified threshold value of 5, which corresponds to $P_d = 72\%$ and $P_{fa} = 39\%$ on the ROC curve. It can be seen from Figure 6(b) that the target is not completely segmented. This may cause problems when extracting features and trying to classify the ROI as target or non-target based upon the silhouette.

Figures 7 (a)-(c) show examples of false alarms when detecting FOI. False alarms shown include camera lens scratch (Figure 7(a)), and sea bottom features (Figures 7(b) and 7(c)). The false alarms generated in these data sets tend to be less solid and have less regularity in their shape. Therefore, it may be possible to reduce the false alarm by imposing a regularity criterion.

VI. Conclusions & Future Work

This paper described and analyzed a block-based detector for detecting underwater targets. Using the block-based detector the log-likelihood ratio is computed for each block within all frames in a run. Overall a detection rate of 100% can be achieved at the cost of a false alarm rate of 50% over all runs using this block-based detection method.

The main challenge, however, is that a good ROI must be generated before feature extraction, in addition to reducing the number of false alarm rate. Additionally, detection of partial targets and classification based on partial silhouettes may also pose major challenges. An important benefit of the proposed detector lies in the fact that detection of FOI and ROI segmentation can be achieved in a single step. This FOI detection coupled with automatic ROI segmentation will reduce the number of objects from which features need to be extracted, as well as reducing the overall load on the classifier. Although FOI detection and automatic ROI segmentation are desirable benefits further work is needed in order to fine-tune and improve the ROI segmentation. More specifically, a robust object silhouette definition needs to be developed while reducing the number of objects extracted from each frame. This is the key to successful object classification and identification. The algorithms developed in this research provided good results for underwater target detection from CCD EO imagery. Among the desirable characteristic of the proposed methods is also the simplicity of the algorithm for detecting FOI in a run, while automatically segmenting the ROI of mine-like objects. Unlike the methods in [1], no preprocessing is needed here and one algorithm is used for both FOI identification and ROI extraction.

Future work includes using Zernike moments [10], [14], [15] as shape dependent features for classification of the detected objects in this data set. Work is devoted to extraction of shape dependent feature from segmented ROI. These Zernike moments will be used as object features due to their rotational and translational invariance as well as robustness to noise. Further work will also be devoted to development of a GUI application for training and using the detection and classification systems.

Acknowledgment

This work is supported by Applied Signal Technology, Inc. (AST), Torrance, CA under contract #261-0137. The authors would like to thank Dr. Kent Harbaugh from AST for providing the data for this study and technical support.

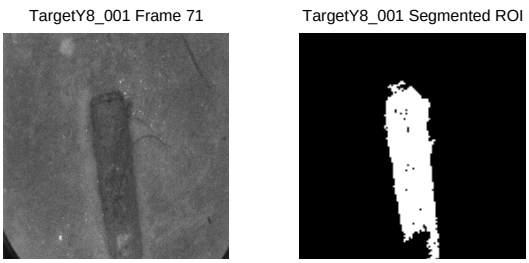

(a) Easy

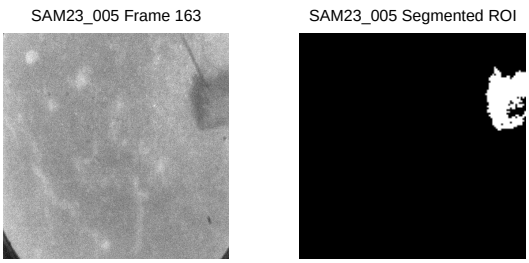

(b) Medium

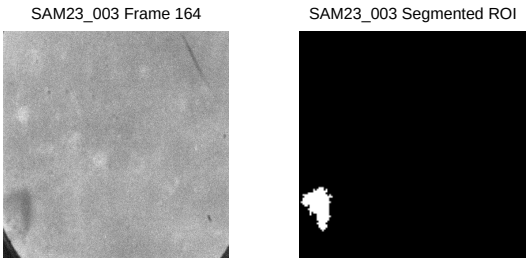

(c) Difficult

Fig. 6. (a) Detection example 'easy target' TargetY8_001. Left: FOI, Right: detection result. (b) Detection example 'medium target' SAM23_005. Left: FOI, Right: detection result and (c) Detection example 'difficult target' SAM23_003. Left: FOI, Right: detection result.

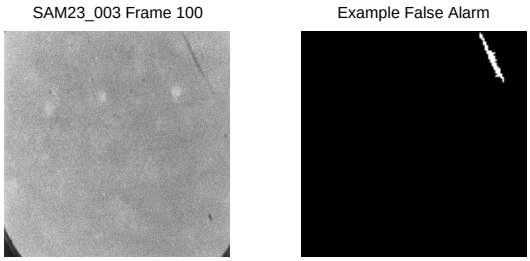

(a) Lens Scratch

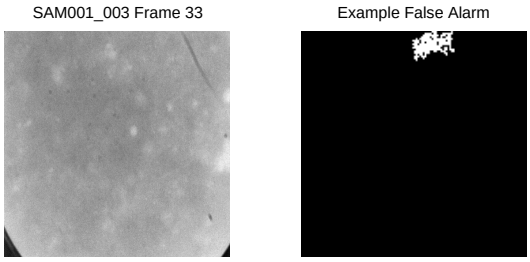

(b) Ocean bottom features

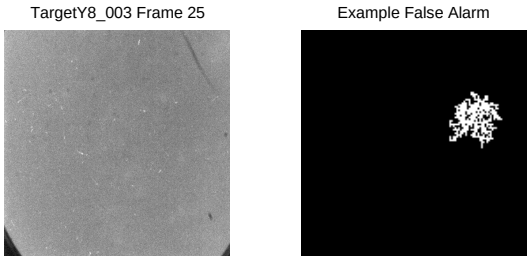

(c) Ocean bottom features

Fig. 7. (a) Detection false alarm example camera lens scratch SAM23_003. Left: FOI, Right: detection result. (b) Detection false alarm example sea bottom SAM001_003. Left: FOI, Right: detection result and (c) Detection false alarm example sea bottom TargetY8_003. Left: FOI, Right: detection result.

REFERENCES

[1] G. Tao, M. Azimi-Sadjadi, and A. Nevis, "Underwater target identification using GVF snake and zernike moments," *OCEANS 2002*, vol. 3, pp. 1535–1541, October 2002.

[2] A. Gleckler, "Multiple-slit streak tube imaging lidar (MS-STIL) applications," *Proc. SPIE*, vol. 4035, no. 1, pp. 266–278, April 2000.

[3] M. P. Strand, "Underwater electro-optical system for mine identification," *Proc. SPIE*, vol. 2496, no. 1, pp. 487–497, April 1995.

[4] E. Watson, "New imaging modalities for laser-based systems," *IEEE Proceedings: Aerospace Conference*, vol. 3, pp. 1593–1599, March 2001.

[5] J. Salazar and M. Azimi-Sadjadi, "Identification of underwater mines from electro-optical imagery using an operated-assisted reinforcement on-line learning," *OCEANS 2003*, vol. 1, pp. 124–131, April 2003.

[6] M. D. Iwanowski, "Surveillance unmanned underwater vehicle," *OCEANS '94*, vol. 1, pp. I/116–I/119, September 2004.

[7] J. J. Shirron and T. E. Giddings, "A model for the simulation of a pulsed laser line scan system," *OCEANS '06*, vol. 1, pp. 1–6, September 2006.

[8] A. Nevis, J. S. Taylor, and B. Cordes, "A baseline object detection algorithm using background anomalies for electro-optic identification sensors," *Proc. of 2002 MTS/IEEE Oceans Conference, Biloxi*, vol. 3, pp. 1546–1554, October 2002.

[9] J. S. Taylor and M. C. Hulgan, "Electo-optic identification research program," *Proc. of 2002 MTS/IEEE Oceans Conference, Biloxi*, vol. 2, pp. 994–1002, October 2002.

[10] G. Tao, M. R. Azimi-Sadjadi, and A. Nevis, "Underwater target identification using GVF snake and Zernike moments," *Proc. of the MTS/IEEE Oceans*, vol. 3, no. 11, pp. 1535–1541, Oct 2002.

[11] H. L. Van Trees, *Detection, Estimation, and Modulation Theory Part I*. John Wiley and Sons, 1968.

[12] L. L. Scharf and B. D. Van Veen, "Low rank detectors for Gaussian random vectors," *IEEE Trans. Acoust., Speech, Signal Process.*, vol. 35, no. 11, pp. 1579–1582, Nov 1987.

[13] E. L. Lehman, *Testing Statistical Hypotheses*. New York: Wiley, 1986.

[14] C. Teh and R. Chin, "On image analysis by the methods of moments," *IEEE Trans. on Pattern Analysis and Machine Intelligence*, vol. 10, no. ., pp. 496–513, July 1988.

[15] A. Khotanzad and J. Lu, "Classification of invariant image representation using a neural network," *IEEE Trans. on Acoustics, Speech and Signal Processing*, vol. 10, no. ., pp. 1028–1038, June 1990.